ALEPH 86-48
G. Stimpfl
17.4.1986

Distr.: TPC

KINK SEARCH FOR MUON CANDIDATES IN THE TPC

G. Stimpfl, MPI München

INTRODUCTION

The aim of this note is to show how the detection of the decays of fast ($p > 2$ GeV/c) π's and K's into $\mu + \nu$ can be improved by refining the normal χ^2 test and what one can gain by using the z measurements of the wires and not of the pads.

Chapter 1 shows how the χ^2 value of a track fit can be split into a systematic (non fluctuating) term coming from the kink itself, a statistically fluctuating term due to the measurement errors, and a cross term. The kink contribution can be very well understood by a formula derived for the case of no magnetic field.

Based on the considerations presented in chapter 1, which are also valid in good approximation for slightly curved tracks with a kink (μ candidates), two new methods for kink searches were developped. These new methods are called "condensation" of measurements and the "χ^2 difference test" and are discussed together with the well known χ^2 test and the Run test in chapter 2.

In order to evaluate the power of these methods a track simulation and kink search program was written. It is described in chapter 3.

Finally the results using pad and wire data or pad data only are presented in chapter 4. The efficiencies of the above mentioned tests are compared for π's with momentum $p = 10$ GeV/c (π_{10}) and K's with $p = 5$ GeV/c (K_5). The χ^2 difference test in space with condensation of the wire measurements is found to be most efficient. It is shown how the power of this method varies with momentum and polar angle.

1. Contributions to χ^2 for kinked tracks

A fit to n pairs of measurements (x_i,y_i) with infinite precision in x and resolution σ in y giving n pairs of fitted points (x_i,y_{fi}) has a χ^2 value given by

$$\chi^2 = \sum_{i=1}^{n} (y_i-y_{fi})^2 / \sigma^2 \ . \qquad (1.1)$$

In order to understand how the statistically fluctuating measurement errors and the systematic deviation of a kinked track from a straight fit contribute to χ^2, it is useful to study the case of straight lines with one kink. For fast tracks the r-z (wire) plane of the TPC can be considered as such a case to a first approximation.

We can split the measurements y_i into

$$y_i = y_{si} + y_{ki} + y_{ei} \ , \qquad (1.2)$$

where y_{si} is the result of a straight line fit and y_{ki} the difference between a kinked straight line fit and y_{si} assuming no measurement errors ($\sigma = 0$). y_{ei} takes the finite resolution into account (see fig. 1). Fitting a straight line (non-kink fit) to these measurements means $y_{fi} \approx y_{si}$ and from (1.1) and (1.2) we get

$$\chi^2_{nf} = \sum_{i=1}^{n} (y_{ki} + y_{ei})^2 / \sigma^2 \ , \qquad (1.3)$$

which we can write as

$$\chi^2_{nf} = \chi^2_k + \chi^2_e + \chi^2_{ke} \qquad (1.4)$$

with

$$\chi^2_k = \Sigma_i (y_{ki})^2 / \sigma^2 \qquad (1.5)$$

$$\chi^2_e = \Sigma_i (y_{ei})^2 / \sigma^2 \qquad (1.6)$$

$$\chi^2_{ke} = 2\ \Sigma_i (y_{ki} y_{ei}) / \sigma^2 \ . \qquad (1.7)$$

1.1 Error term

The error term χ^2_e has, for gaussian errors, a χ^2 distribution with n_{df} = n-2 degrees of freedom and depends therefore on n only. The expectation value and variance

$$E[\chi^2_e] = n_{df} \tag{1.8}$$
$$Var[\chi^2_e] = 2n_{df} \tag{1.9}$$

lead to the normal standard deviation

$$SD[\chi^2_e] = (\chi^2_e - n_{df}) \; / \; \surd \; 2n_{df} \; . \tag{1.10}$$

Normalizing χ^2_e by $1/n_{df}$

$$X^2_e = 1/n_{df} \times \chi^2_e \tag{1.11}$$

gives

$$E[X^2_e] = 1$$
$$Var[X^2_e] = 2/n_{df} \tag{1.12}$$
$$SD[X^2_e] = (X^2_e - 1) \; / \; \surd \; (2/n_{df}) \; .$$

For n = 300 we get

$$\sigma[X^2_e] = \surd \; Var[X^2_e] = \surd \; (2/n_{df}) = 0.08 \; . \tag{1.13}$$

1.2 Kink term

For linear least squares fits, assuming small decay angles and many equidistant measurements with constant resolution, the following formula for the kink contribution was derived

$$\chi^2_k = 4/3 \times n/\sigma^2 \times L^2 \tan^2(\psi/2)/\sin^2\vartheta \times v^3(1-v)^3 \; . \tag{1.14}$$

n is the number of measurements, σ the resolution, L the track length between the first and the last measurement, ψ the decay angle, ϑ the polar angle, and v the distance between the first measurement and the decay point divided by L ($0 \leq$

$v \leq 1$). Since we measure the pairs (r_i, z_i) in the TPC we have $L = \Delta r/\sin\vartheta$ and therefore $\chi^2_k \propto 1/\sin^4\vartheta$.

The function

$$f(v) = v^3(1-v)^3 \tag{1.15}$$

is shown in fig. 2. It has a maximum of $2^{-6} = 0.016$ for $v = 1/2$ and a mean value $E[f(v)] = 0.007$.

Assuming $\sigma = 0.11$ cm, $\Delta r = R(pad_{21}) - R(pad_1) = 130.8$ cm, and $\tan(\psi/2) \approx \psi/2$ we obtain

$$X^2_k = 1/n \times \chi^2_k = 0.47\ f(v)\ \psi^2\ \text{mrad}^{-2}\ /\ \sin^4\vartheta\ . \tag{1.16}$$

For $f(v) = E[f(v)] = 0.007$ and $\vartheta = \pi/2$ we get

$$X^2_k = 3.3\ 10^{-3}\ \psi^2\ \text{mrad}^{-2}. \tag{1.17}$$

This means that for $\psi = 1$ mrad the kink contribution X^2_k is about 24 times smaller than the R.M.S. of the error term $\sigma[X^2_e]$ (1.13). In the following we shall indicate the momentum of the tracks by an index (π_{10} means a π with momentum p = 10 GeV/c). For the maximum decay angle of $\pi_{10} \rightarrow \mu + \nu$, which is 4 mrad, and n = 300 we get

$$X^2_k = 0.053 = 0.7\ \sigma[X^2_e]\ . \tag{1.18}$$

1.3 Cross term

The cross term has the expectation value 0. Its fluctuations are less than those of χ^2_e. With n = 300 and $\sigma = 0.11$ cm we find $\sigma[X^2_{ke}] = 0.032$ and 0.043 for π_{10} and π_5, respectively.

Fig. 3 shows the relative densities of the normalized χ^2 contributions X^2 for π_5 without magnetic field. Since X^2_e and X^2_{ke} are symmetric around their mean value of 1 and 0, respectively, X^2_e is shifted by 1 to the left. The density of X^2_k is scaled by 1/2.

2. Kink tests

2.1 Normal χ^2 test

This method consists in fitting a non-kinked track to the data and cutting on the obtained χ^2 value. As we can see from (1.4) and (1.18), the efficiency of this test for decaying π's is rather poor because the fluctuations of the errors are bigger than the contribution of the kink.

2.2 Run test

The χ^2 test deals only with the absolute value of the fit residuals. For kinked tracks we expect that the signs are not randomly distributed. A method which takes only the signs of the residuals into account is the Run test [1], where a run denotes a sequence of residuals of the same sign.

In the Run test we count the number of runs r, the number of positive signs n_1, and and the number of negative signs n_2. We consider the number r of runs as a test variable with the following mean value E, variance Var, and normal standard deviation SD [1]

$$\begin{aligned} E[r] &= 2n_1n_2/n + 1 \\ Var[r] &= 2n_1n_2 \times (2n_1n_2-n) \,/\, n^2(n-1) \\ SD[r] &= (r-E[r]) \,/\, \sqrt{Var[r]} \\ &\text{with} \quad n = n_1 + n_2 \ . \end{aligned} \tag{2.1}$$

From the SD value we can deduce the probability that the signs are randomly distributed.

Since the information used in the run test and in the χ^2 test are the signs and the absolute values of the fit residuals, respectively, the two methods are complementary and can therefore be used together. The combined probability is given by [1]

$$P = P_{\chi^2}P_r \,(1 - \log P_{\chi^2}P_r) \ , \tag{2.2}$$

where P_{χ^2} and P_r are the probabilities of the fit for the χ^2 and Run tests, respectively. Although this equation is only valid for continuous distributions, it can also be used as an approximation for the discrete run test.

For the studied tracks the power of the run test is limited by two facts

- if the systematic deviations due to the kink are smaller than the resolution, the distribution of the signs of the residuals will remain almost random.
- If these deviations are big compared to the resolution almost all kinks can be found by the χ^2 test alone. The decays which escape detection have a topology (very small decay angle or near to the edges) for which the absolute value and the signs of the residuals are not significantly different from those of a straight track.

2.3 χ^2 test with condensation

By going from many (n_1) measurements to fewer (n_2) measurements with higher resolution, a process we call "condensation", the error is reduced by

$$\sigma_2/\sigma_1 = \sqrt{(n_2/n_1)} \ . \qquad (2.3)$$

It follows from (1.9) and (1.14) that $\sigma[\chi^2_e] = \sqrt{\mathrm{Var}[\chi^2_e]}$ is decreased by the factor $\sqrt{(n_{df1}/n_{df2})}$ whereas χ^2_k remains unchanged. Therefore χ^2_k is enhanced on average with respect to χ^2_e.

As we shall see in chapter 4 this method is quite efficient if we use the z measurements of the wires instead of the pads.

2.4 χ^2 difference test

For those decays, where the deviations of the kinked track from a straight track are not bigger than the measurement errors, the methods described so far are not powerful enough. From (1.4) and fig. 3 we see that the weakness of the χ^2 test comes from the large fluctuations of the error term χ^2_e. We therefore should try to eliminate χ^2_e.

If we make a kink fit we have $y_{fi} \approx y_{si} + y_{ki}$ and from (1.2), (1.1), and (1.6) we get

$$\chi^2_{kf} = \Sigma_i (y_{ei})^2 \ / \ \sigma^2 = \chi^2_e \ . \qquad (2.4)$$

This is analogous to the case of a non-kink fit to a track which does not decay, since in both instances only the errors contribute to χ^2.

We can therefore eliminate the error term by fitting the data twice, once with a non-kinked track (χ^2_{nf}) and once with a kinked track (χ^2_{kf}), and subtracting the resulting χ^2 values. From (1.4) and (2.4) we get

$$\Delta\chi^2 = \chi^2_{nf} - \chi^2_{kf} = \chi^2_{k} + \chi^2_{ke} \ . \qquad (2.5)$$

Since we don't know the position of the kink we have in fact to fit the data several times with different kink radii in order to get χ^2_{kf}. The minimum χ^2 value gives us χ^2_{kf}.

Instead of cutting on χ^2 like in the normal χ^2 test we can now cut on $\Delta\chi^2$. The sensitivity of this method, which I propose to call the "χ^2 difference test", is limited only by the fluctuations of χ^2_{ke} and the quality of the fit, i.e., the difference between the real and the fitted track.

$\Delta\chi^2$ does not vanish for non-decaying tracks since the kink fit and the non-kink fit will give slightly different results due to the measurement errors. Fig. 4 shows the probability (in percent) that a track fit gives a ΔX^2 ($= 1/n_{df}\ \Delta\chi^2$) value less than that indicated in the abscissa. If we cut for example at $\Delta X^2 = 0.04$ we miss about 5% of the K_S decays and about 50% of the π_{10} decays whereas the contamination from non-decaying tracks is less than 0.5%.

3. Kink search on simulated tracks

3.1 TPC simulation

Since our aim is the comparison of different kink search methods we are allowed to make a number of simplifying assumptions which characterize the bulk of the expected data. Difficulties arising with real data (small ϑ, missing points, confused tracks, etc.) are excluded here.

The following assumptions were made:

- decays occur only between pad row 1 (R_1 = 39.8 cm) and pad row 21 (R_{21} = 170.6 cm);
- 300 wire measurements (r_i, z_i) for each track which are equally spaced between the first and the last pad row ($r_1 = R_1$, $r_{300} = R_{21}$);
- homogeneity in φ;
- no multiple scattering;
- gaussian errors;
- constant pad rφ resolution of $\sigma_{r\varphi}$ = 0.02 cm;
- constant wire z resolution of σ_{zw} = 0.11 cm;
- pad z resolution of $\sigma_{zp} = \sqrt{[\sigma_{zw}^2 + (0.12 \text{ cm } \cot\vartheta)^2]}$.

3.2 Track simulation

The decays $\pi^\pm \rightarrow \mu^\pm + \nu$ and $K^\pm \rightarrow \mu^\pm + \nu$ were studied in detail for π/K momenta of p_1 = 5 and 10 GeV/c and polar angles ϑ between 40° and 90°. In this ϑ range measurements are obtained from all pad rows and wires. A momentum cut was applied at p_μ = 2 GeV/c because μ's with smaller momentum are stopped in the iron between the TPC and the muon detector.

In order to show the momentum dependence also tracks with 3 GeV/c $\leq p_1 \leq$ 50 GeV/c were generated and analyzed.

3.3 Track fits

In the TPC the tracks follow a helical path. The x-y (r-rφ) projections (= pad plane) of the helices are circles. The motion in the r-z projection (= wire plane) can be described by

$$z(r) = 2\rho \arcsin(r/2\rho)\ \mathrm{ctg}\vartheta + z_0 \ , \qquad (3.1)$$

ρ being the radius of curvature in x-y and z_0 a constant displacement.

3.3.1 Non-kink fit

Since z(r) depends on ρ we first have to fit a circle to the x-y measurements giving us ρ_f. We can rewrite (3.1) as

$$\begin{aligned} &z(r) = a \times f(r) + b \\ &\text{with} \quad a = \mathrm{ctg}\ \vartheta \\ &\qquad\ \ b = z_0 \\ &\qquad\ \ f(r) = 2\rho_f \arcsin(r/2\rho_f) \end{aligned} \qquad (3.2)$$

and apply a linear least squares fit with the two parameters a and b to the r-z measurements.

Denoting the χ^2 values of the two fits by $\chi^2_{nf}(xy)$ and $\chi^2_{nf}(rz)$ we have

$$\chi^2_{nf} = \chi^2_{nf}(xy) + \chi^2_{nf}(rz). \qquad (3.3)$$

for the combined fit.

3.3.2 Kink fit

In the x-y plane we fit two circles with one measurement in common, i.e., circle 1 from pad row 1 to pad row i and circle 2 from pad row i to pad row 21. Requiring at least 4 points for each circular fit we go from i = 4 to i = 18 and look for the minimum of $\chi^2_i = \chi^2_{i1} + \chi^2_{i2}$. The minimum gives us the χ^2 value of the kink fit, and the radius of the corresponding pad row ($R_{i,min}$) gives us the r coordinate of the kink

$$\begin{aligned} &\chi^2_{kf}(xy) = \chi^2_{i,min} \\ &r_k = R_{i,min}. \end{aligned} \qquad (3.4)$$

If we use the 300 wire measurements in r-z, we apply the same procedure going from wire i = 20 to wire i = 280 in steps of 10.

If we have 21 threedimensional points, from either the z measurements of the pads or by "condensing" the wire measurements around each pad row to one more precise z measurement for each pad row, we proceed in the same way as described above for the x-y plane. Now χ^2_{i1} and χ^2_{i2} (for the first and the second part of the track) are the sums of the χ^2 values obtained in the x-y and r-z plane, respectively,

$$\chi^2_{ij} = \chi^2_{ij}(xy) + \chi^2_{ij}(rz) \qquad (j = 1,2)$$
$$\chi^2_{i} = \chi^2_{i1} + \chi^2_{i2} \; .$$

4. Results

Although the study was carried out for π's and K's with momenta p_1 = 5 and 10 GeV/c and several polar angles ϑ we shall concentrate on the results obtained for the two extreme cases, namely π's with p_1 = 10 GeV/c (π_{10}) and K's with p_1 = 5 GeV/c (K_5). π_{10} have a maximum decay angle of ψ_{max} = 4 mrad and K_5 of ψ_{max} = 114 mrad (222 mrad without p_μ cut). All results except fig. 6 are averages over ϑ between 40° and 90° where tracks are measured in the full TPC.

The following tests were applied to the simulated data:

- normal non-kink fit with χ^2 test [N]
- condensation of the wire measurements and non-kink fit with χ^2 test [C]
- condensation of the wire measurements and non-kink fit with χ^2 and Run test [C+R]
- condensation, non-kink fit, and kink fit with $\Delta\chi^2$ test [C+Δ].

Table 1 shows a comparison of the efficiencies of these methods in the pad plane (x-y), in the wire plane (r-z), and in space (x-y-z). The percentage of detected kinks is called "kink search efficiency" (KSE). A cut at x % means that x % of the tracks without decay are incorrectly found to have a kink.

We see that the biggest improvement in the r-z plane is achieved by "condensation" of the wire measurements [C]. If we apply in addition the Run test [C+R], the efficiency is increased by about 2.5% for π_{10} and remains almost the same for K_5. The use of the χ^2 difference method [C+Δ] instead of the combination of the χ^2 test and the Run test gives a much better result for π_{10}. For K_5 this test is slightly less efficient since its sensitivity near to the edges is smaller. This is because the difference between the kinked track and the kink fit is bigger near the edges since we need at least 4 measurements for each of the two circle fits.

Table 2 contains the results using only pad information and no wire data for the track fits.

A comparison between the KSE of the χ^2 difference test in space given in Table 1 and 2 shows that the KSE for π_{10} and K_5 is increased by about 15% and 5%, respectively, if one uses the wire measurements in the r-z plane.

Table 1: Kink search efficiencies [%] using pad and wire data

cut	0.5%				5%			
method	N	C	C+R	C+Δ	N	C	C+R	C+Δ
π_{10}								
x-y	25.0	25.0	27.5	34.0	36.0	36.0	39.0	45.5
r-z	4.5	21.0	23.5	35.0	14.0	34.0	37.0	47.0
x-y-z	14.0	35.0	36.5	50.0	26.5	47.0	49.5	60.5
K_5								
x-y	87.0	87.0	87.5	89.5	90.0	90.0	90.5	92.0
r-z	78.5	88.5	88.5	90.5	82.5	91.0	91.0	92.5
x-y-z	91.0	95.5	95.5	94.0	93.0	96.5	96.5	95.0

Table 2: Kink search efficiencies [%] using pad data only

cut	0.5%		5%	
method	C	C+Δ	C	C+Δ
π_{10}				
x-y	25.0	34.0	36.0	45.5
r-z	1.0	1.5	6.5	9.5
x-y-z	21.5	34.5	33.0	46.0
K_5				
x-y	87.0	89.5	90.0	92.0
r-z	65.5	72.5	72.5	78.0
x-y-z	91.0	88.5	93.0	90.5

Some features of the best method, the χ^2 difference test in space with condensed wire measurements, are presented in fig. 5 - 8. The momentum dependence of the KSE for π's and K's in the range p_l = 3 - 50 GeV/c is shown in fig. 5. The dependency of the KSE on ϑ for π_{10} and K_5 can be seen in fig. 6. A plot of the decay angle ψ versus the kink radius r_k for (a) detected and (b) missed kinks is presented in fig. 7 for π_{10} and in fig. 8 for K_5. For π_{10} the full ψ range is shown, whereas for K_5 a cut at 20 mrad is applied in order to see the behaviour for small decay angles in more detail. The shape of the plots for the detected kinks (a) can be very well understood by the function $f(v) = v^3(1-v)^3$, which describes the dependence of the kink contribution on the decay radius (see fig. 2).

5. Conclusion

Several kink-detection methods for $\pi\pm$ and $K\pm$ decaying into $\mu\pm + \nu$ inside the TPC were studied on simulated data. The "χ^2 difference test" in space combined with the "condensation" of the wire data was found most powerful and is therefore proposed as kink search algorithm in the TPC. This method will be evaluated further, adding ITC and vertex information.

The results also show that the use of wire data instead of the z measurements from the pads increases the kink search efficiency substantially.

Reference

[1] W.T. Eadie et al., Statistical Methods in Experimental Physics, Amsterdam : North-Holland, 1971.

FIGURE CAPTIONS

1. Schematic of a kinked track. y_{si} is the result of a straight line fit, y_{ki} the difference between a kinked straight line fit and y_{si} assuming infinite resolution, and y_{ei} the measurement error.

2. Function $f(v) = v^3(1-v)^3$ for $0 \leq v \leq 1$.

3. Relative densities of X^2_e, X^2_k, and X^2_{ke} for π_5 and no magnetic field. Since X^2_e and X^2_{ke} are symmetric around their mean value of 1 and 0, respectively, X^2_e is shifted by 1 to the left. The density of X^2_k is scaled by 1/2.

4. Integrated ΔX^2 distribution for decaying π_{10} and K_5 and for tracks without kink.

5. Kink search efficiency of the χ^2 difference test with condensation versus momentum for π and K averaged over ϑ.

6. Kink search efficiency versus polar angle ϑ for π_{10} and K_5.

7. Decay angle versus kink radius of π_{10} for the cases where the decay was found (a) or escaped detection (b).

8. Decay angle versus kink radius of K_5 for the cases where the decay was found (a) or escaped detection (b).

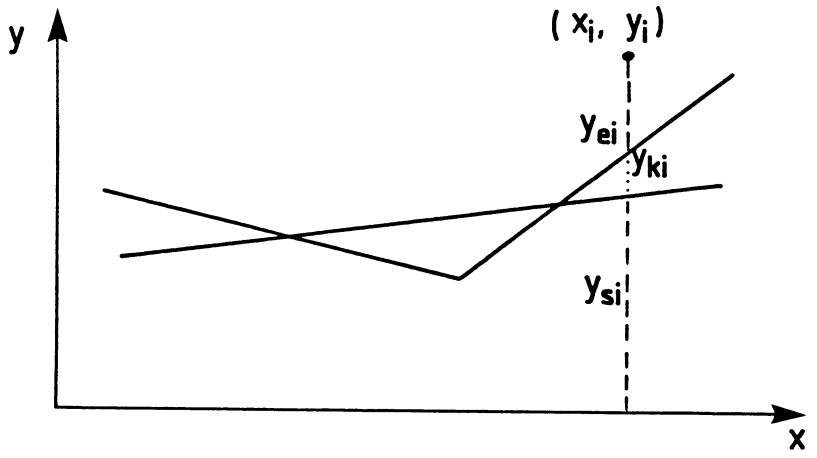

Fig. 1: Schematic of a kinked track.

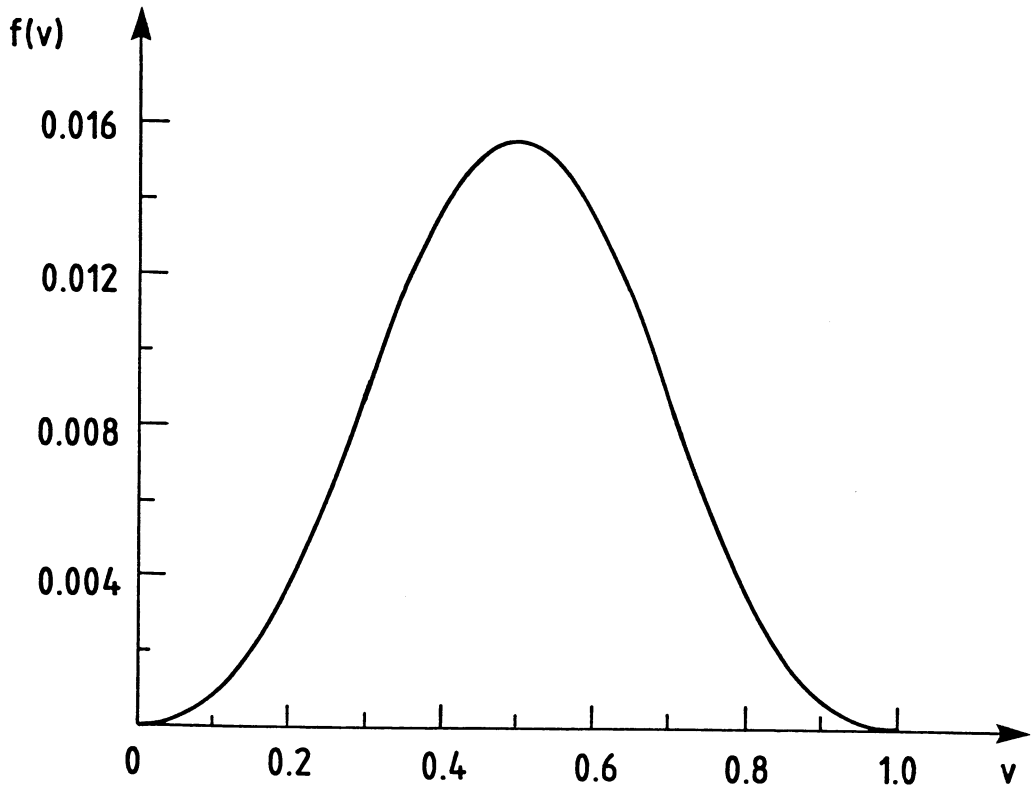

Fig. 2: Function $f(v) = v^3(1-v)^3$.

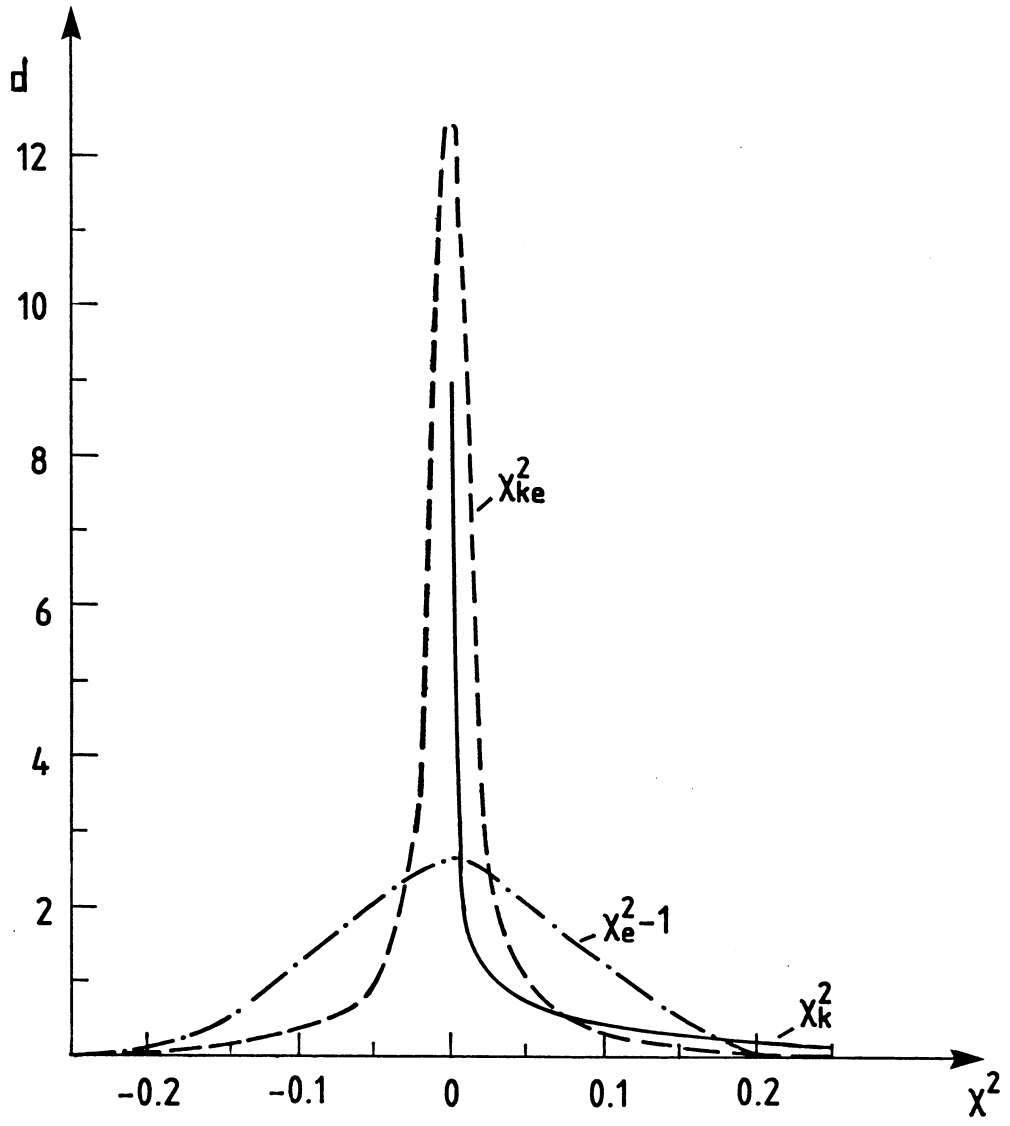

Fig. 3: Relative densities of X^2_e, X^2_k, and X^2_{ke} for π_5 and no magnetic field.

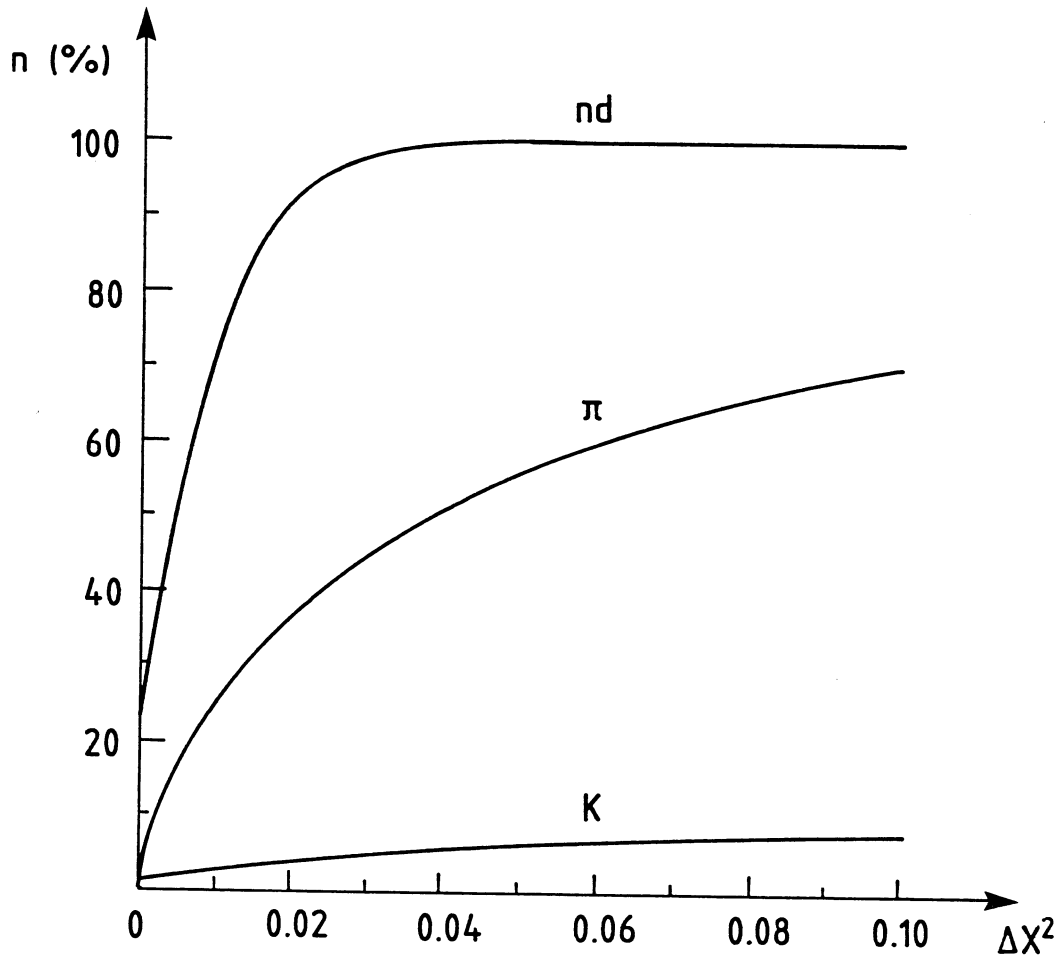

Fig. 4: Integrated ΔX^2 distribution for decaying π_{10} and K_5 and for tracks which do not decay (nd).

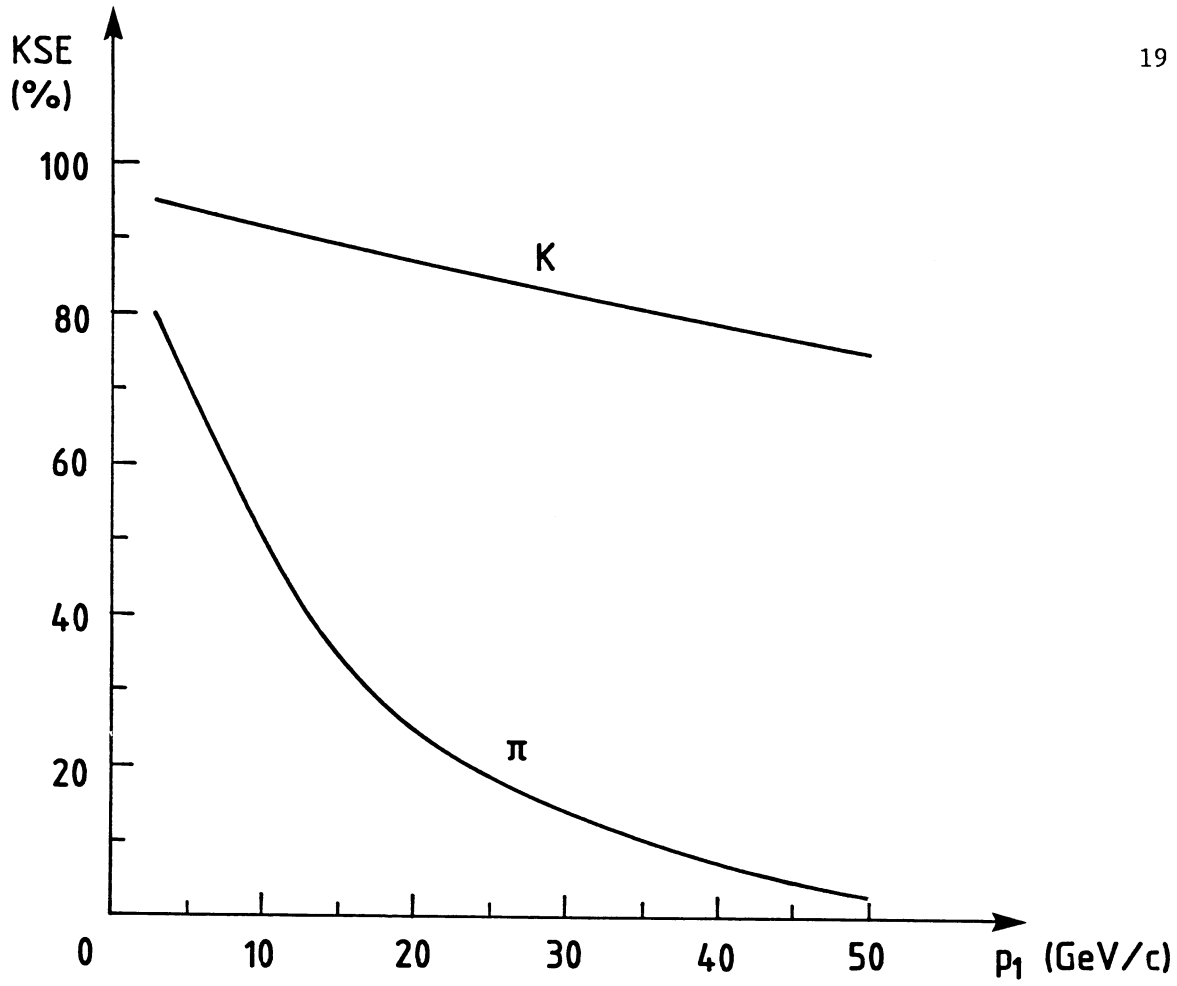

Fig. 5: Kink search efficiency versus momentum for π and K.

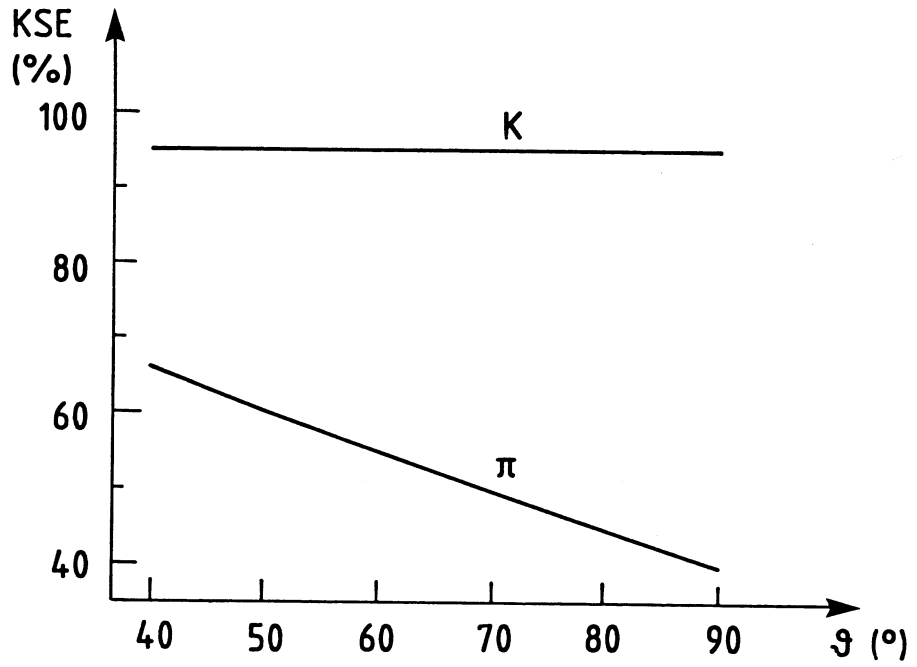

Fig. 6: Kink search efficiency versus polar angle ϑ for π_{10} and K_5.

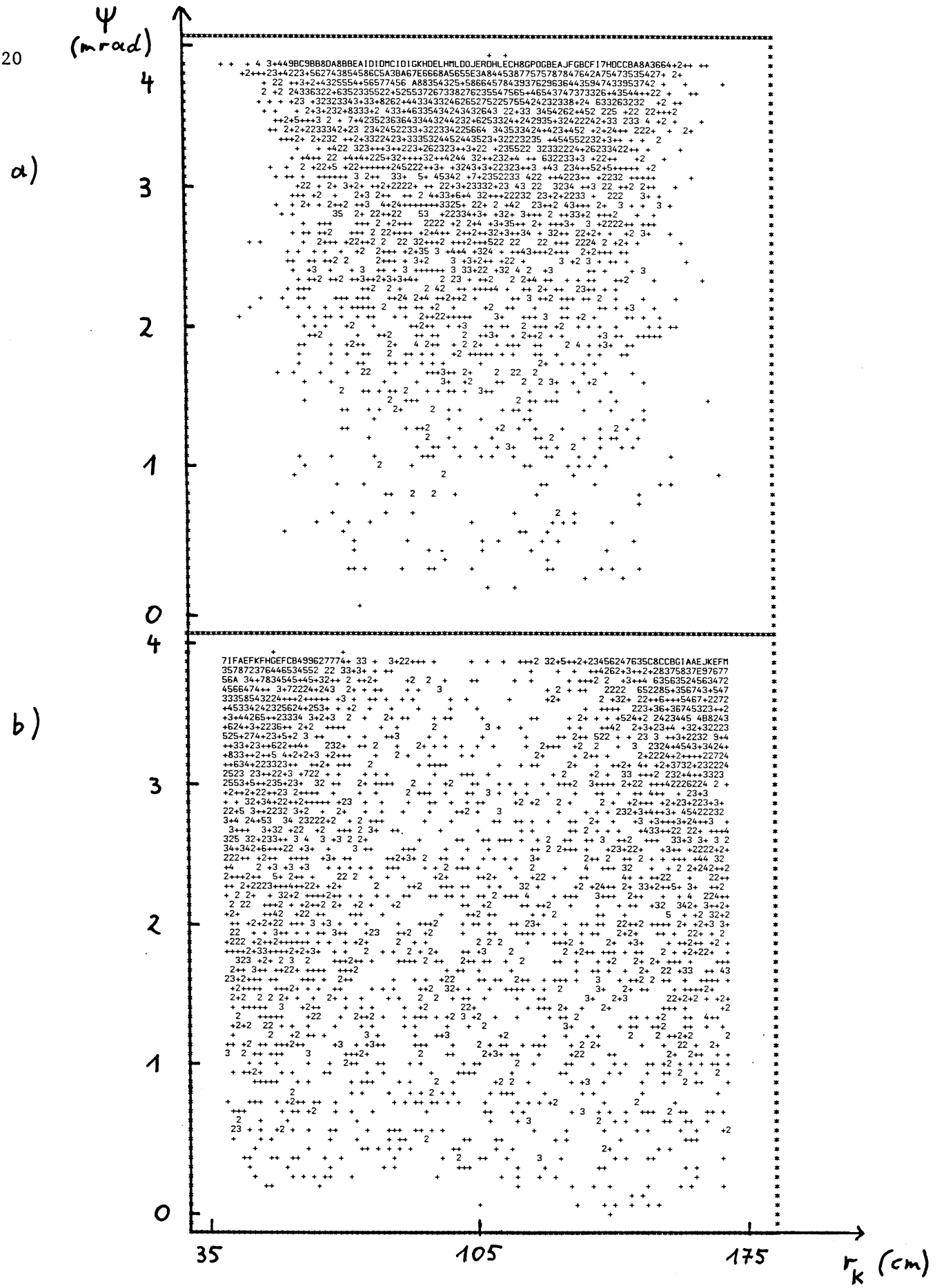

Fig. 7: Decay angle versus kink radius for π_{10}:
a) kink detected, b) kink not detected.

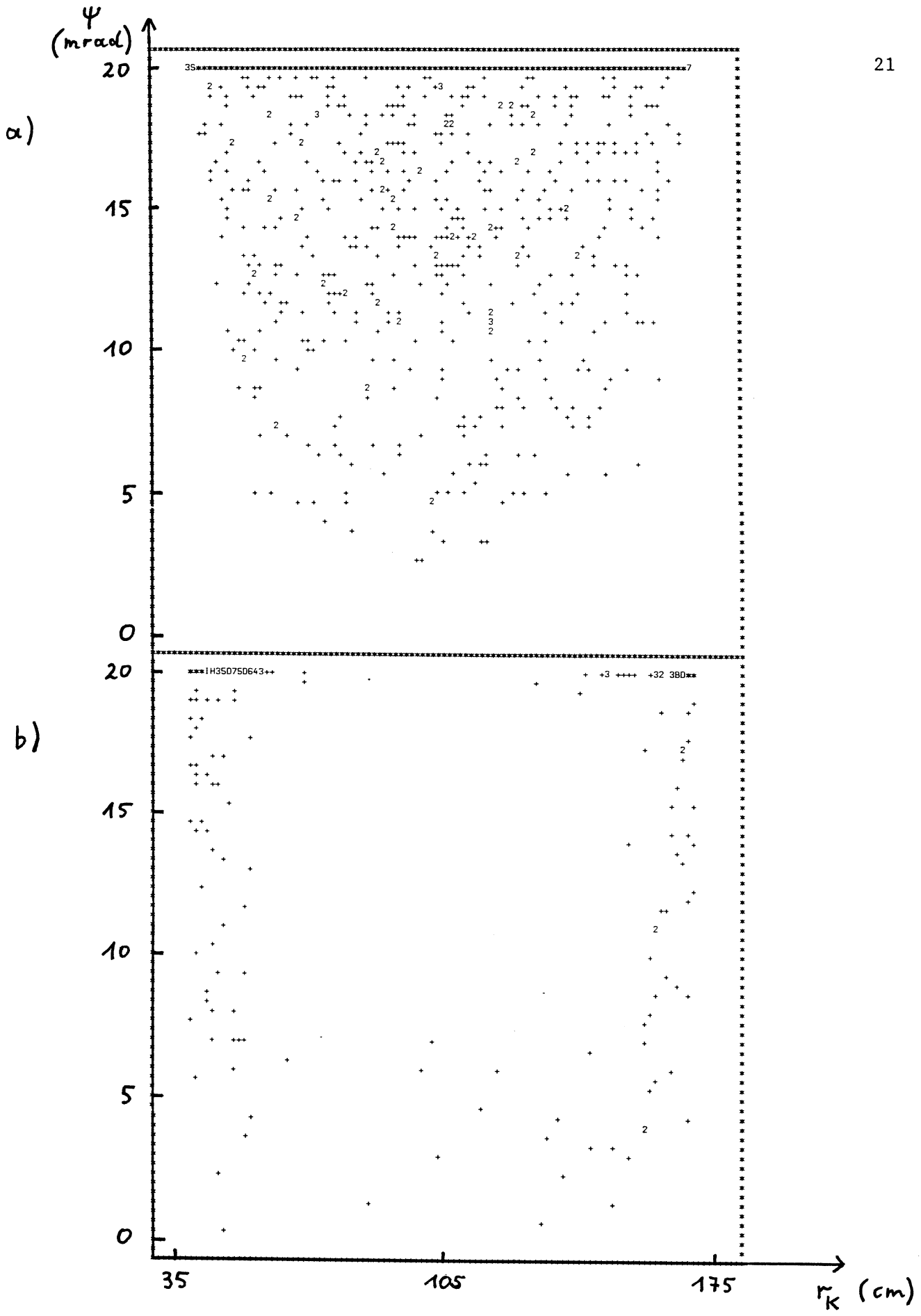

Fig. 8: Decay angle versus kink radius for K_S:
a) kink detected, b) kink not detected.